Introduction

The surface-level interaction between harmful pathogens such as *Escherichia coli* (*E. coli*) and solid materials is a global healthcare problem that lacks comprehensive understanding. Catheter-associated urinary tract infection is the source of nearly 20% of episodes of healthcare-associated bacteremia in acute care settings, and nearly 50% of episodes of bacteremia in long-term care facilities[1]. Furthermore, indwelling catheters provide a surface for the attachment of bacterial adhesins, thereby enhancing microbial colonization and the formation of biofilms[2]. This gap in knowledge amplifies the difficulty of establishing pertinent safety protocols and preventative measures to halt the spread of infections. Therefore, my research group is engineering nanoscale materials (i.e., nanopatterned surfaces) with diblock copolymer systems to shed light on the surface-level interactions. For example, we previously used a polystyrene-*block*-poly(methyl methacrylate) (PS-*block*-PMMA) diblock copolymer to fabricate vertically oriented cylindrical PS structures (i.e., "PS nanopillars") on silicon substrates. The results demonstrated that the PS nanopillars exhibited highly effective bactericidal and bacteria releasing properties (i.e., "dual properties," illustrated in **Figure 1**) against *E. coli* for at least 36 hours (h) of immersion in an *E. coli* well plate[3]. Our overarching goal is to help establish the physical (i.e., morphological) and mechanical basis of bacteria resistance.

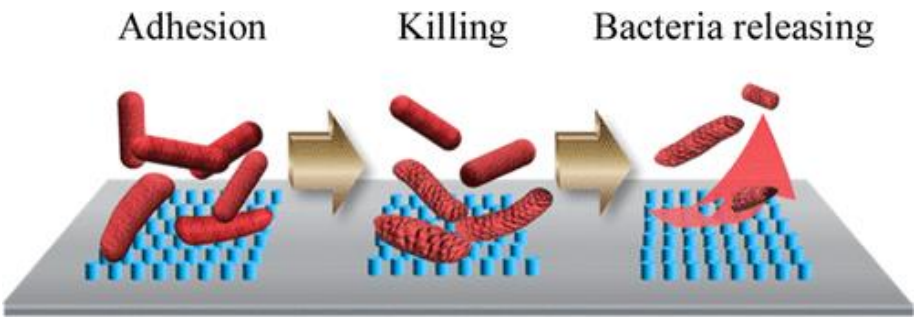

Figure 1. Demonstrated surface interaction pathway for bacterial cells and other biological contaminants with PS nanopillars.

Objectives

The primary objective of this project was to develop a robust image analysis pipeline to evaluate the efficacy of anti-biofouling surface coatings against *E. coli*. We have hundreds of data sets that consist of fluorescence microscopy images, so evaluating each image by performing an ensemble of manual pre/post-processing measures through external software(s) is not feasible. Namely, the Jython macro we developed some time ago requires images to be opened sequentially on a user's system through the ImageJ command window while analysis routines are taking place. Though the macro is functional, it captures many artifacts from the instrument that are not part of a real sample. We need an automated pipeline, preferably one that can be run without such extensive dependencies, runs efficiently, and applies a reasonable background filter. The data (i.e., the number of stained cells) extracted from each image will be

used to complement ongoing experimental (i.e., *in-situ* atomic force microscopy) and computational studies (i.e., molecular dynamics (MD) simulations) of the surface phenomena.

Contributions

For this independent project, I executed critical tasks spanning the entire workflow:

- Developed Python scripts (convertTo8Bit.py and StarDist_cmd.py) for pre/postprocessing and processing, respectively
- Interfaced ImageJ (win-64) headlessly from the command line
    - Integrated a verbose output option for cmd-displayed status updates
- Configured a StarDist 2D model with (tunable) default parameters
- Used os to manage an input and output directory
    - These handled preprocessed 8-bit images (from ImageJ) and postprocessed label images (from StarDist), respectively
    - Wrote the total number of cell counts per image to an external data file in the output directory
- Assessed results qualitatively (segmentation algorithm accuracy) and quantitatively (performance compared to manual analysis)

Tools and Techniques

Experimental methods and sample data

We leveraged *in-situ* staining techniques with the cell-permeable Hoechst 33342 dye and propidium iodide (PI) in our recent work to enhance the visualization of cell nuclei in fluorescence microscopy images[3]. The images were captured using a high-resolution EVOS microscope. The sample medium consisted of *Escherichia coli* (E. coli), a common bacterium used in biology research due to its well-characterized genome and cellular structure. For analysis, I selected a specific set of sample data to test the effectiveness of our imaging and segmentation approach. This included 5 images of PS nanopillars coated with titanium dioxide (TiO_2) after 36 h of immersion. We previously observed that the strongest dual bactericidal and bacteria-releasing properties were emerged by the TiO_2-coated PS nanopillars [3]. Additionally, I used 5 control images which featured an empty *E. coli* well to serve as a baseline for comparison after 36 h. This setup helped in assessing the contrast between the treated and untreated conditions, thus providing a clearer insight into the efficacy of the TiO_2 coatings. **Figure 2** shows an example of an image from each data set to help visualize both conditions.

Core software and packages

StarDist[4,5,6], a deep learning plugin for Fiji (ImageJ), was used for the segmentation of cell nuclei from fluorescence microscopy images. The plugin is based on convolutional neural

networks and excels in accurately predicting the complex shapes of nuclei. Developed under the CSBDeep framework, StarDist leverages a novel approach using star-convex polygons for segmentation. This allows for precise boundary delineation even in densely clustered cellular environments, a significant advantage over traditional (i.e., manual) segmentation methods that often struggle with overlapping objects.

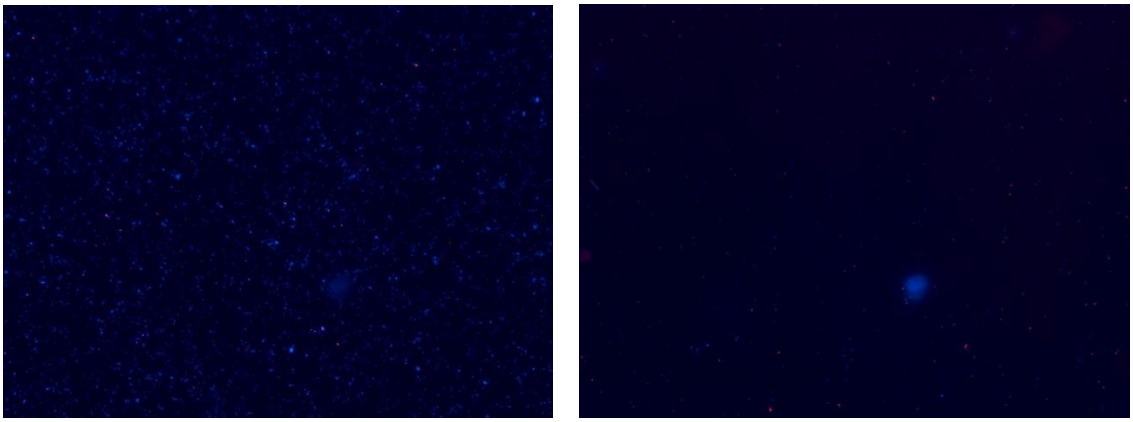

Figure 2. Example of empty *E. coli* well (left; corresponding to control sample) and dry surface of TiO_2-coated PS nanopillars (right; corresponding to experimental sample) after 36 h.

CSBDeep, the parent project of StarDist, is a collection of deep learning solutions designed to enhance image restoration, segmentation, and object classification within the bioimaging community. The framework provides a generic architecture based on U-Net-like neural networks tailored for various microscopy image analysis tasks. CSBDeep's methodology emphasizes careful training with low amounts of noisy labeled data, facilitating robust performance even under challenging imaging conditions. For this project, I imported pretrained models and the **normalize** function from the CSBDeep Python package, which prepares images for neural network processing by standardizing pixel intensity values and enhancing contrast.

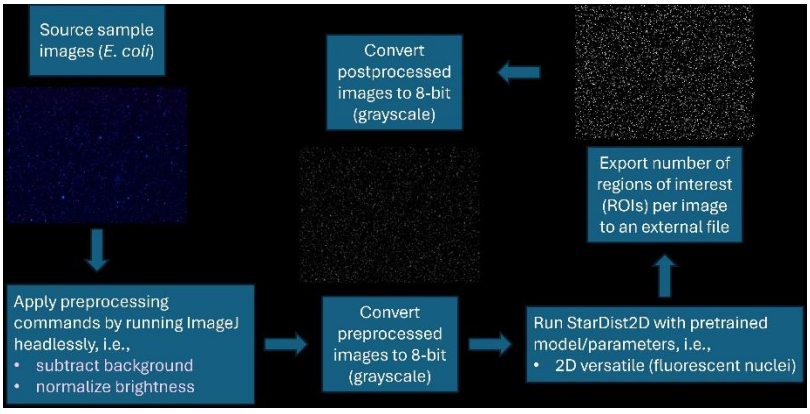

Figure 3. Workflow of pre/postprocessing routines that are invoked with cmd. Label images are also converted to 8-bit at the end for ease of comparison with preprocessed 8-bit images.

Specifically, the StarDist 2D model **"2D_versatile_fluo"** was employed. The model has been optimized for fluorescent nuclei, which satisfies our purpose of counting stained *E. coli* from

images. **NumPy** was used to count the regions of interest (ROIs) per image. This analysis allowed for assessing the prevalence and distribution of segmented nuclei across the two sample treatment conditions. Finally, The decision to use **version 1.54f (June 2023) of Fiji (ImageJ)** for implementing StarDist was necessitated. The more recent 1.54i (March 2024) version exhibited significant issues related to stability and compatibility with StarDist features.

Workflow

The analysis pipeline is detailed in **Figure 3** for convenience and can be run from cmd using the following command:

```
python StarDist_cmd.py "path\to\ImageJ.exe" "path\to\unprocessed\images"
"path\to\preprocessing\script" "path\to\preprocessed\images"
"model_folder_or_pretrained_name" "path\to\postprocessed\images" -v
```

The analysis begins with a collection of source sample images of *E. coli*. These images are first processed by **convertTo8Bit.py**, which converts every image in a directory to 8-bit grayscale. This conversion is essential for standardizing the images for subsequent analysis. In conjunction with the conversion, ImageJ is run headlessly from cmd using the **'--headless'** flag to apply a set of preprocessing commands, that is, subtracting the background to mitigate any uneven illumination or camera noise and normalizing brightness to ensure a uniform intensity scale for all of the images. Preprocessing is crucial for accurately visualizing the cell nuclei. After preprocessing, the images are fed into the **StarDist_cmd.py** script, which invokes StarDist2D with the **pretrained "2D_versatile_fluo" model**. Once the segmentation is complete, the script quantifies the analysis by exporting the number of regions of interest (ROIs), which represent individual segmented nuclei, for each image to an external data file. This quantification step transforms the image data into a numerical format that can be used for further statistical analysis or to track changes over different sample conditions.

Results and Conclusions

Segmentation quality

The quality of segmentation achieved by even the pretrained StarDist 2D model was commendable. The segmentation results clearly differentiated between the control and experimental samples, with the control sample exhibiting a higher count of segmented nuclei in each of the 5 instances. **Table 1** outlines the difference between the counts per image in each sample condition. This observation aligns with our experimental results that PS nanopillars exhibit good bactericidal and bacteria-releasing properties, which would accordingly result in fewer counts for the experimental sample. The model was also proficient in screening out large microscopy artifacts (**Figure 4**), thus maintaining the integrity of the data. However, an area

identified for potential refinement is the model's inclusion of cell debris in the control sample counts alongside the nuclei (**Figure 4**). This suggests that the model could be adjusted to more selectively capture only viable nuclei, improving the specificity of the segmentation.

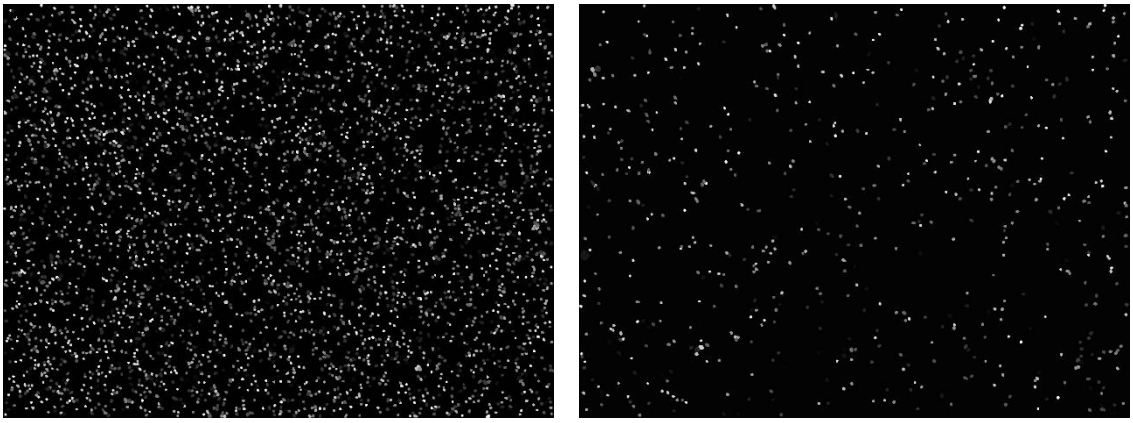

Figure 4. Segmented label image for control (left) and experimental sample (right) after 36 h.

Nevertheless, this issue of cell debris inclusion is more about optimizing the model than a fundamental flaw. The overall trends observed are consistent with expectations and would likely remain unchanged even if all debris were excluded from the analysis. From a research perspective, it is probably more pragmatic to seek a balance that prioritizes the relative significance of the observed trends over absolute accuracy. Such an approach would focus on maintaining the robustness of comparative results across samples, while acknowledging and accommodating the presence of some level of non-nuclei elements within the segmented data.

Table 1. Comparison of ROIs from images between sample conditions

ROIs extracted from control images	ROIs extracted from experimental images
3899	647
3856	688
3829	466
3867	483
3915	447

Performance

The automated workflow reduced the start-to-finish processing time to an impressive 7.5 seconds per image. This is a 97.5 percent decrease in elapsed time compared to the manual workflow. The next phase of the project involves a comparative analysis between the automated and manual segmentation results. This step is crucial to ensure that the relative differences in nuclei counts for the same images remain within an acceptable range. While the automated workflow significantly accelerates the process, the manual script will be maintained

for interactive debugging. This allows for adjustments, such as fine-tuning the brightness settings for image sets with darker backgrounds and ensuring that the automated process remains adaptable to highly variable imaging conditions. Ultimately, the project's worth extends beyond time efficiency. The greatly enhanced precision in image segmentation paves the way for more detailed investigations into biofouling resistance trends on polymer surfaces.

Use cases

The versatility of the developed image analysis pipeline extends well beyond its initial application of processing images of *E. coli* cells on solid surfaces. The script's robust design allows it to handle a diverse array of fluorescent nuclei images by simply modifying the StarDist model and fine-tuning some normalization parameters. This adaptability is rooted in the script's headless functionality, which facilitates seamless transitions between different image processing tasks without the need for user intervention during runtime. Whether the focus is on different bacterial species, mammalian cells, or any fluorescently stained nuclei, the script can be customized to meet the specific requirements of varied experimental setups.

References

1. Greene, L., Marx, J., & Oriola, S. (2008). Guide to the Elimination of Catheter-Associated Urinary Tract Infections (CAUTIs). *Developing and Applying Facility-Based Prevention Interventions in Acute and Long-Term Care Settings*.
2. Jacobsen, S. M., Stickler, D. J., Mobley, H. L., & Shirtliff, M. E. (2008). Complicated catheter-associated urinary tract infections due to Escherichia coli and Proteus mirabilis. *Clinical microbiology reviews*, *21*(1), 26-59.
3. Salatto, D., Huang, Z., Benziger, P. T., Carrillo, J. M. Y., Bajaj, Y., Gauer, A., ... & Koga, T. (2023). Structure-based design of dual bactericidal and bacteria-releasing nanosurfaces. *ACS Applied Materials & Interfaces*, *15*(2), 3420-3432.
4. Schmidt, U., Weigert, M., Broaddus, C., & Myers, G. (2018). Cell detection with star-convex polygons. In *Medical Image Computing and Computer Assisted Intervention–MICCAI 2018: 21st International Conference, Granada, Spain, September 16-20, 2018, Proceedings, Part II 11* (pp. 265-273). Springer International Publishing.
5. Weigert, M., Schmidt, U., Haase, R., Sugawara, K., & Myers, G. (2020). Star-convex polyhedra for 3D object detection and segmentation in microscopy. In *Proceedings of the IEEE/CVF winter conference on applications of computer vision* (pp. 3666-3673).
6. Weigert, M., & Schmidt, U. (2022, March). Nuclei instance segmentation and classification in histopathology images with stardist. In *2022 IEEE International Symposium on Biomedical Imaging Challenges (ISBIC)* (pp. 1-4). IEEE.